Stop A3/3

PICHLER SECTION (GAMS)

Michael Wagreich, Hans Egger, Holger Gebhardt, Omar Mohamed

Topic:
Paleocene/Eocene-boundary in a deep-water turbidite setting

Tectonic unit:
Northern Calcareous Alps

Lithostratigraphic unit:
Gosau Group, Zwieselalm Formation

Chronostratigraphic units:
Upper Paleocene to Lower Eocene

Biostratigraphic units:
Calcareous Nannoplankton Zones NP9 and NP10

Location:
Southern tributary of the Gamsbach (Krautgraben) to the west of Haid (Gams, Styria)

Coordinates:
014° 50′ 26″ E, 47° 39′ 49″ N

References:
Egger et al., 2009; Wagreich et al., 2011.

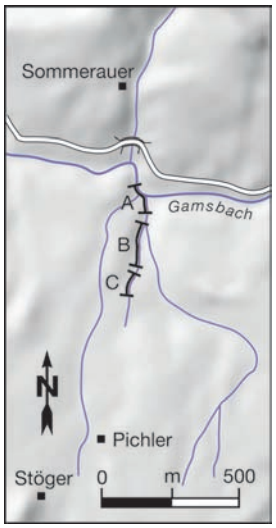

Figure A3.10 ◄
Sketch map indicating detailed location of the investigated sections A, B, and C.

In the area of Gams, the Danian deposits of the Nierental Formation are characterized by the predominance of red and grey pelagic to hemipelagic marlstones and marly limestones with thin turbidites and single debris flows (Egger et al. 2004, 2009a). This interval is followed by a turbidite-dominated unit assigned to the Zwieselalm Formation (Wagreich et al. 2009). Within this formation, a continuous Paleocene/Eocene boundary section is exposed in a creek in the eastern part of the Gams basin (Egger et al., 2009; Wagreich et al., 2011).

The creek forms a southern tributary of the Gamsbach (Krautgraben) to the west of Haid, south of farm house Sommerauer. The base of the Pichler section is located at the confluence of the Gamsbach and the tributary creek including the cut bank of the Gamsbach itself (section A, Fig. A3.10; Fig. A3.11) with a ca. 34 m thick section. Above a few meters covered by debris and vegetation, a continuous, ca. 43 m-thick section starts within the western branch of the creek (section B, Fig. A3.10), which

includes the Paleocene/Eocene boundary interval indicated by the presence of the dinoflagellate cyst *Apectodinium augustum* and the calcareous nannoplankton species *Discoaster araneus*. Additionally, a negative carbon isotope excursion can be interpreted as the CIE-interval at the base of the Eocene. Using the isotope and paleontological records the thickness of the CIE-interval can be estimated as at least 40 m.

Overlying section B, above a 10 m unexposed interval, section C exposes another 27 m of section. The top is overlain by Quaternary moraine.

Figure A3.11 ▲
Section A at the bank of the Gamsbach

Lithology

The Pichler section is dominated by sandy to silty turbidites. Significant differences in rock composition result from variations in carbonate content and the presence and absence of conspicuous marl layers. Based on these features, a lower carbonate-bearing and coarser grained interval can be recognized, followed by a carbonate-poor, finer-grained interval around the Paleocene/Eocene boundary that again grades into a more carbonate-rich interval at the top of the section (Fig. A3.12). Transitions from one interval to the other occur over several meters to tens of meters. Therefore, no exact positions of boundaries between those facies types can be given within the section.

The lowermost ca. 13 m of the section (section A, outcrop at cut bank of Gamsbach) are characterized by several up to 110 cm-thick sandy turbidites with clear grading from a gravel-dominated base (components up to 7 cm) to a fine sandstone/siltstone top. Bouma intervals T_a to T_e are present, sometimes with prominent convolute lamination (Fig. A3.13). The sandy parts of the turbidite beds grade within a few centimeters into dark grey silty claystones. Thin turbidite

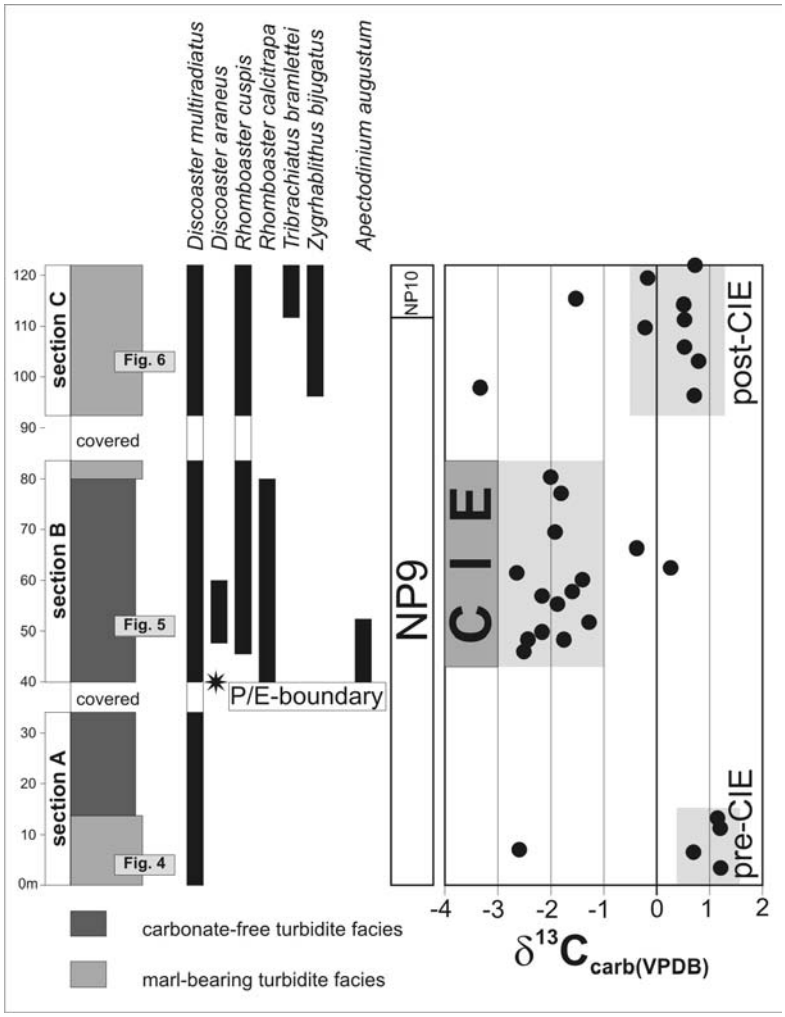

Figure A3.12 ▲
Detailed composite overview log of the studied section with sections A, B and C marked, main biostratigraphic markers (nannofossils, dinoflagellates) recognized, and carbon isotope data of bulk carbonate. Positions of detailed sections of figs. 4 to 6 indicated in log.

sandstone to coarse siltstone beds (0.5 to 30 cm) are present between these thick beds which constitute the majority of the turbidites present. Thicker beds display complete Bouma sequences whereas thin beds mostly show the Bouma interval T_{cde}. Amalgamation of several turbidite beds to single thick beds is a common feature. Some clasts of Paleocene platform limestones are present in the turbidite layers.

A 15 cm-thick mud-supported debris flow bed with a silty-clayey matrix and clasts up to 5 cm in diameter is present. Another conspicuous feature of this basal part are up to 80 cm-thick marl beds (mean carbonate content of five samples 12.4 wt%, maximum 16.7 wt%) without any visible bedding. The top parts of these marl beds as well as some of the dark grey thin silt-clay layers show downward bioturbation by mainly *Chondrites*-type burrows. Sandstone/pelite ratios are between 1:1 to 2:1. The turbidites, especially the thin sandy layers, display only weak cementation due to a low carbonate content. Turbiditic shales are dark grey, mainly only a few centimeters thin, and largely devoid of carbonate. No clear fining- or coarsening-upward cycles could be recognized; only at meter 5 of the section a 1 m-thick succession of six amalgamated turbidite beds display a fining-upward and thinning-upward trend.

The turbidite facies is characterized by classical sandy turbidites showing both complete and incomplete, base-truncated Bouma sequences. This corresponds to facies C and D of Walker (1978) and, according to the classification of Pickering et al. (1989), these sandstones fall into the classical turbidite facies C2 (organized sand-mud couplets – classic turbidites). The thick sandstone beds show characteristics for transitional deposition from relatively low- to high-concentrated and high-density turbidity currents. The dark grey clays are interpreted as representing the fine-grained portion of the turbidites. The thicker marl beds present may be interpreted either as (fine-grained) turbidites or hemipelagites. Several observations argue for an origin as a turbidity current: (1) these marl beds follow directly above turbiditic sandstone beds, (2) at 2.5 m in the section 15 cm-thick pebbly mudstone directly grades into

Figure A3.13 ▼
Detailed sedimentological log from the lower part of section A (4.00 to 8.00 m; white m denotes marl beds) and photographs of typical facies types from this section (arrows point to position of photographs within the section).

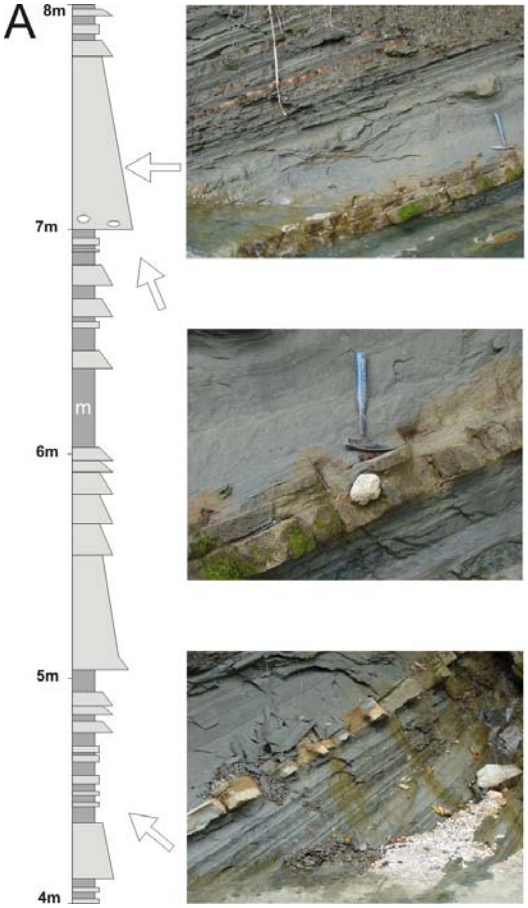

Figure A3.14 ▼
Detailed sedimentological log from the middle part of section B (59.00 to 63.00 m; white m denotes reddish marl bed) and photographs of typical facies types from this section (arrows point to position of photographs within the section).

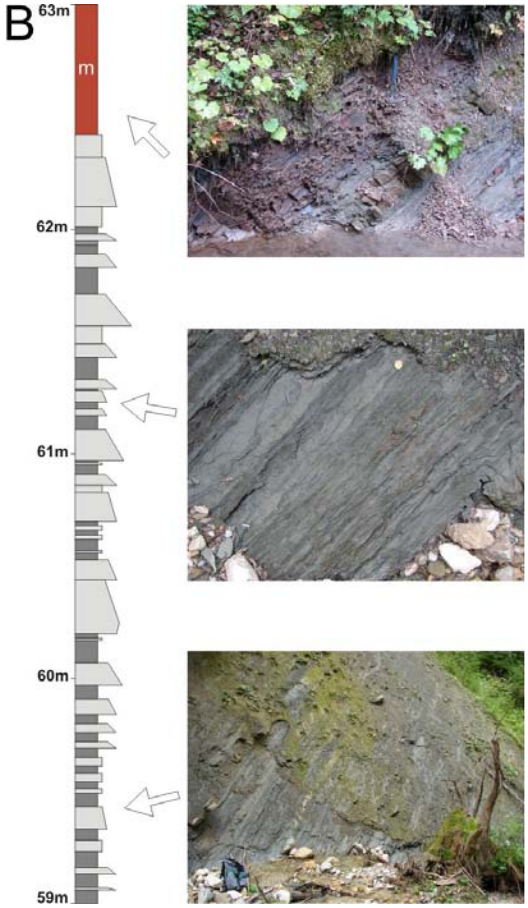

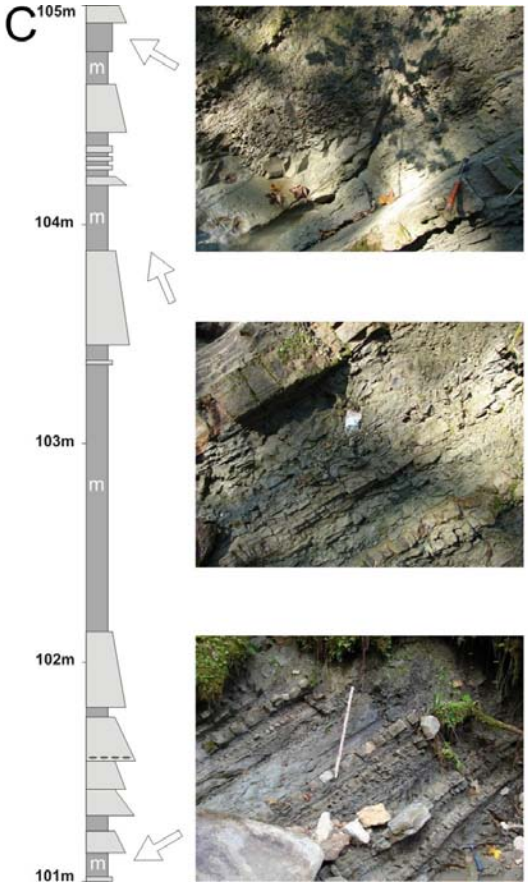

Figure A3.15 ◄
Detailed sedimentological log from the middle part of section C (101.00 to 105.00 m; white m denotes marl bed) and photographs of typical facies types from this section (arrows point to position of photographs within the section; scale in lower right 90 cm).

a 80 cm-thick marl bed; (3) foraminiferal data also support a transported microfauna and thus argue against a hemipelagic deposition of these marl beds.

This marl-bearing interval grades in the top part of section A into an interval without distinctive marl beds, which ranges up to the upper part of section B, up to ca. section meter 80. There, thin-bedded sandy- to silty turbidites with thin, dark-grey silty claystone intervals prevail. Claystones to marly claystones have carbonate contents of 0 to 6.4 wt% (mean of 28 samples 1.9 wt%). A few sandstone beds up to 48 cm are present but the majority of sandstone layers are only a few centimeters thin. Grading is ubiquitous and thicker sandstones show complete T_{a-e} Bouma sequences; thinner beds often show only T_{cd} intervals. Two distinctive reddish brown marly claystone to marl beds (22.9 and 34.2 wt% carbonate content) of up to 85 cm thickness are present at 62 and 66 m of the section. Bioturbation has only very rarely been observed.

Sandstone/pelite ratios are between 2:1 to 5:1.This facies is interpreted as mainly thin-bedded classical turbidites in the sense of Walker (1978: facies D) and Pickering et al. (1989; facies C2.2 and C2.3). The lack of identifiable hemipelagic layers and the high proportion of sand suggests a high-frequency turbidite environment. The reddish claystone layers probably also represent turbidites, i.e. mud turbidites, as also suggested by a transported and poor microfauna (see below).

A prominent feature of the Paleocene/Eocene-boundary interval are siderite concretions, which are conspicuous in outcrops due to their hardness and rusty color (Fig. A3.16).Concretions occur within several levels both in sandy-silty and in silty-clayey material, especially in the middle part of the section. Both, layers enriched in disseminated siderite cement and platy to rounded ellipsoid siderite nodules

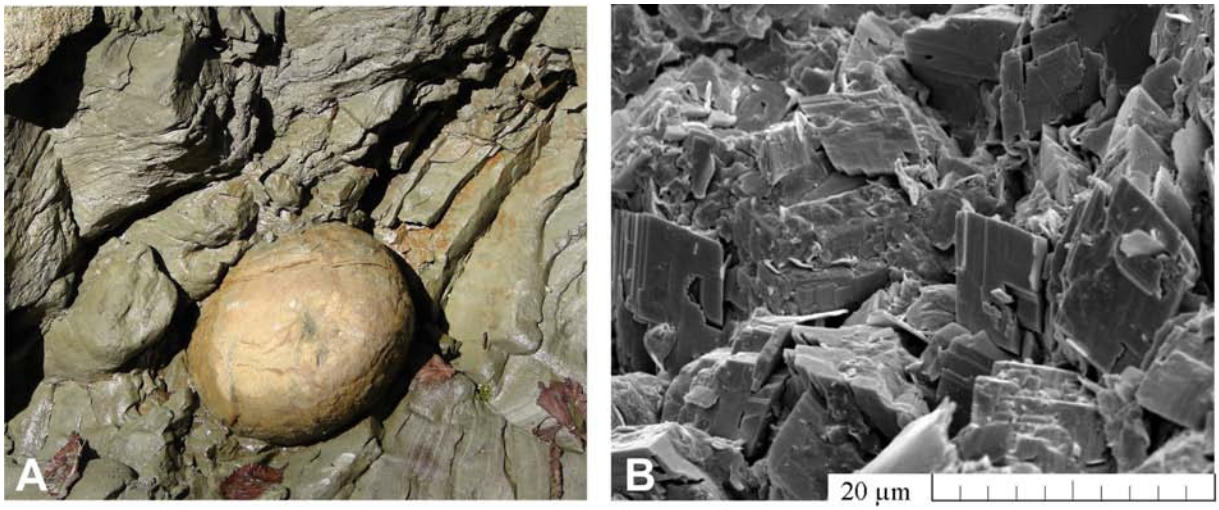

Figure A3.16 ▲
Siderite concretion (13 cm in diameter), outcrop in middle part of section B, within largely carbonate-free turbidites. 7B. REM picture of diagenetic siderite from concretion in section B.

up to 30 cm in diameter are present. Siderite ranges up to a maximum of 66 wt% within the concretions (41.1 wt% FeO). Mudstones embedding the concretions show FeO values around 6–8 wt%. No significant enrichment in minor elements was observed. A pre-compaction origin of the concretions is evident by the presence of squeezed sedimentary layering around the nodules. Although detailed investigations are missing, an early diagenetic origin of the siderite is probable (e.g. Laenen & De Craen 2004).

Starting at around 80 m in the section, light grey to slightly greenish grey marly claystones and marl beds again occur and become significant, and sandstone beds become thicker again (up to 80 cm). This facies resembles largely the basal interval; however, the carbonate contents rises significantly: the mean of nine samples of marl layers above 90 m in the section is 19.7 wt% and the maximum is 29.0 wt%. Although cm-thick sandstone turbidite beds are still present, thicker sandstones and marls predominate the topmost part of the section above 100 m. Convolute bedding and structures indicative of water-escape processes such as flame and ball-and-pillow structures are often present in the sandstones. Amalgamation of beds is commonly observed. Flute casts indicate a paleotransport direction from SW to NE. Marl beds up to 120 cm thick are intercalated. Foraminiferal data indicate that at least some of the marl beds represent hemipelagites as suggested by an autochthonous foraminiferal assemblage with abundant planktic foraminifera.

Carbon isotope stratigraphy

Stable isotope measurements of whole-rock samples (Fig. A3.12) are influenced by diagenesis and the small amount of carbonate of the samples, which can be as low as 0.1%. The oxygen isotope values range between -1.0 and -5.5‰ and are considered to be strongly influenced by diagenesis as no systematic variation could be recognized within the section. Carbon isotope values range from +1.2 to -8.9‰. This large variation is considered to be also influenced by diagenesis and the low carbonate content and highly negative values below -8‰ are not considered further. However, except for a few outliers, a clear trend can be seen in the section. The lower part (up to 15 m) is characterized by values around 0.5‰ (mean of six samples 0.43‰). A gap with virtually no carbonate occurs up to ca. 45 m. The following ca. 40 m-thick interval is characterized by slightly negative values around -2‰ (mean of 15 samples -1.7‰). After another gap due to a covered section interval, above 90 m, values increase again to ca. 0.5‰ (mean of 10 samples -0.14‰).

Based on these data and the extended stratigraphic range of marker species we speculate that the CIE of the PETM (e.g. Zachos et al. 2007) is represented by a strongly expanded section of at least 35 ms and present between 45.7 and 80 m. As no isotope data are available from the 33 m-thick interval below 45.7 m due to the lack of carbonate and a covered section interval, the CIE may well comprise an interval thicker than 35 m.

Biostratigraphy

The biostratigraphic evaluation of the Pichler section is handicapped by the presence of two unexposed intervals, the paucity of carbonate especially in the middle part of the section, and the predominance of turbidites, which result in mostly allochthonous microfossil assemblages. Therefore, both calcareous nannofossil biostratigraphy and especially planktic foraminiferal zonations had to be applied with caution. In addition, some of the samples, especially around the suspected P/E-boundary, were also tested for dinoflagellates. The characteristic dinoflagellate *Apectodinium augustum* (Fig. A3.17) was found in several samples from 40 to 52.50 m (Fig. A3.12), a clear indicator of the P/E-boundary interval (Egger et al. 2000; Crouch et al. 2001; Sluijs et al. 2006,

Figure A3.17 ▲
Apectodinium augustum (Harland, 1979) Lentin & Williams, 1981, a dinoflagellate typical for the Paleocene/Eocene-boundary interval; Pichler section, 40 m. Scale bar = 20 µm.

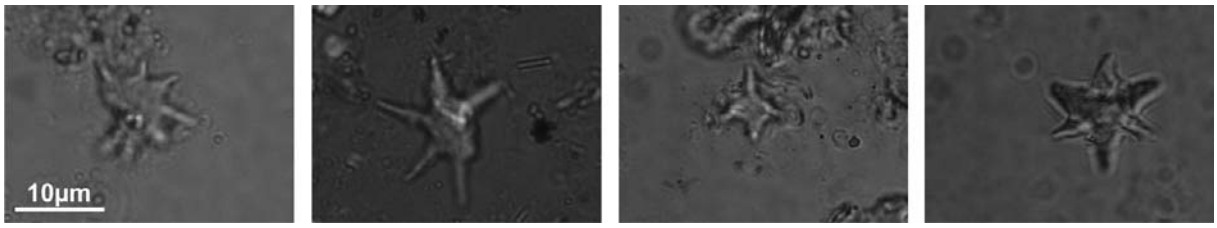

Figure A3.18 ▲
Nannofossil marker species from the Pichler section (light microscope, magnification 1000x, all same scale): A. *Discoaster araneus* Bukry, 1971(sample PE4-07, 57.62 m), B. *Rhomboaster calcitrapa* Gartner, 1971 (sample PE7-07, 51.66 m), C. *Rhomboaster cuspis* Bramlette & Sullivan, 1961 (sample PE14-08, 109.50 m), D. *Tribrachiatus bramlettei* (Brönnimann & Stradner, 1960) Proto Decima et al., 1975 (sample PE18-08, 115,14 m).

2007b, 2008), thus providing additional biostratigraphic information for the nearly carbonate-free interval at the base of section B.

The distribution of nannofossil marker species (Fig. A3.18) indicates the presence of the *Discoaster multiradiatus* Zone (Zone NP9) and the *Tribrachiatus contortus* Zone (Zone NP10) in the the Standard Tertiary zonation of Martini (1971) (Fig. A3.12). In the lower part of the section *Discoaster multiradiatus* occurs regularly. Above a 6 m long unexposed interval, the first *Rhomboaster calcitrapa* was found at 40.40 m and the first *Rhomboaster cuspis* at 45.70 m. The first occurrence of the genus *Rhomboaster* is in the upper third of Zone NP9 and coincides with the onset of the CIE-interval (e.g. Aubry 1996) and, therefore, is a good tool to recognize the P/E-boundary. Another indicator for the CIE-interval is the asymmetrical *Discoaster araneus* whose stratigraphic range is restricted to this interval (e.g. Tremolada & Bralower 2004). *Discoaster araneus* appears for the first time at 47.76 m and ends at 59.92 m of the section. *Zygrhablithus bijugatus,* a holococcolith species, has its first occurrences in the upper part of Zone NP9 (Bown 2005) but becomes common not before the P/E-boundary (Bralower 2002). At the Pichler section, this species is common from 96.20 m to the top of studied section. The base of NP10 was identified by the first appearance of *Tribrachiatus bramlettei* at 110.90 m.

Only two samples are considered to represent almost completely autochthonous foraminiferal assemblages. Sample PEG-36 from near the base of the section at 10.3 m contains a number of rather large agglutinated foraminifera (Fig. A3.19). Some of the species provide limited biostratigraphic control in flysch deposits (Geroch & Nowak 1983). *Reophax subnodulosus* points to an Eocene age.

Sample PEG-05 from the upper portion of the section at c. 110.96 m contains a number of planktic foraminifera that were used for age classification (Fig. A3.20). In particular the concurrent presence of the species *Subbotina velascoensis, Acarinina soldadoensis, Morozovella acuta, M. aequa, M. apanthesma, M. occlusa, M. gracilis* and *M. subbotinae* point to the latest Paleocene - earliest Eocene planktic Zone P5 (Olsson et al. 1999; Pearson et al. 2006) as defined in Berggren et al. (1995). We could not apply the revised zonation of Berggren & Pearson (2005) because index species such as *Acarinina sibaiyaensis* or *Pseudohastigerina wilcoxensis* were not found in the samples. From the foraminiferal point of view, it remains unclear whether this sample is of Paleocene or of Eocene age. The benthic *Aragonia velascoensis* restricts the youngest possible age to zone P5 (Tjalsma & Lohmann 1983).

Sedimentation rates

Given a 40 m-thick interval that marks the CIE in the Pichler section and the 170 to 210 kyr duration of that interval (Röhl et al. 2000, 2007; Abdul Aziz et al. 2008; Westerhold et al. 2009; Murphy et al. 2010) a sediment accumulation rate of 19 to 23.5 cm/kyr can be calculated. Even higher accumulation rates are calculated by applying shorter duration estimates as reported recently by Sluijs et al. (2007a: 90 – 140 kyrs; see also Westerhold et al. 2009). Accumulation rates can be compared to those from the terrestrial record of the Bighorn Basin, USA (Sluijs et al. 2007a, Abdul Aziz et al. 2008), but are at least one magnitude larger than accumulation rates in pelagic sections, e.g., in the Belluno Basin in northern Italy (Dallanave et al. 2009). By counting the sandy turbidites within this interval (240 layers) a periodicity of ca. 700 yrs (170 kyrs duration) can be reconstructed for turbidity currents entering the basin. The pronounced input of sand fraction is different from most other sections showing the Paleocene-Eocene transition (e.g. Schmitz & Pujalte 2007) and can be interpreted as a result of regional tectonic activity overprinting the effects of global environmental perturbations.

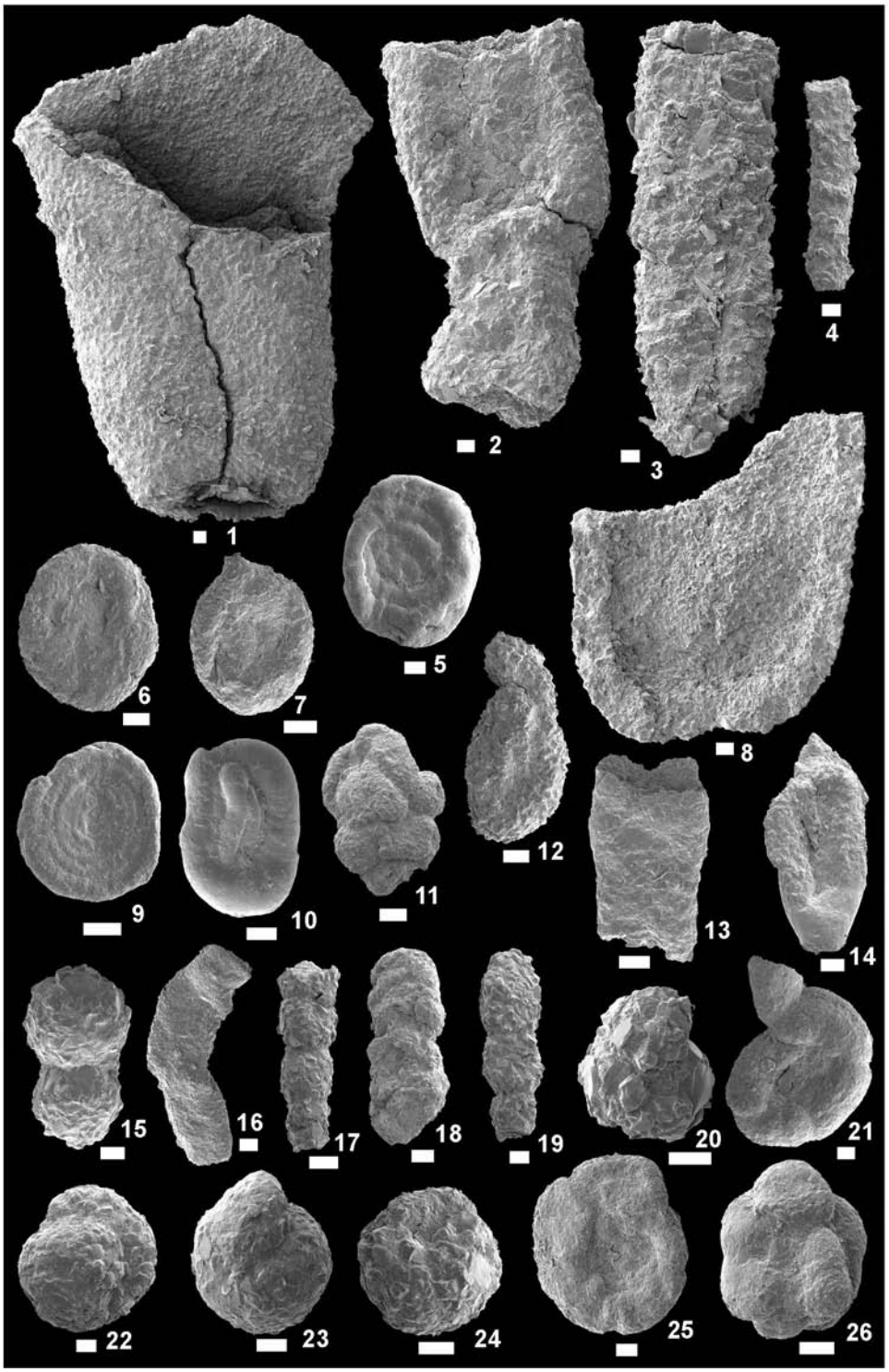

Figure A3.19 ▲
Agglutinated foraminifera
1, **2**, **8**: *Arthrodendron diffusum* (Ulrich, 1904); **3**: ?*Nothi*a sp.; **4**: *Psammosiphonella cylindrica* (Glaessner, 1937); **5**: *Ammodiscus glabratus* Cushman & Jarvis, 1928; **6**: *Psammosphaera fusca* Schulze, 1875; **7**: *Placentammina placenta* (Grzybowski, 1898); **9**: *Ammodiscus siliceus* (Terquem, 1862); **10**: *Glomospirella gaultina* (Berthelin, 1880); **11**: „*Glomospira*" irregularis (Grzybowski, 1898); **12**: *Dolgenia* sp.; **13**: *Kalamopsis grzybowskii* (Dylasanka, 1923); **14**: *Hyperammina* cf. *nuda* Subbotina, 1950; **15**: *Reophax duplex* Grzybowski, 1896; **16**: *Subreophax* sp.; **17**: *Reophax* cf. *minuta* Tappan, 1940; **18**: *Hormosina velascoensis* (Cushman, 1926); **19**: *Reophax subnodulosus* Grzybowski, 1898; **20**: *Trochammina* sp.; **21**: *Trochamminoides dubius* (Grzybowski, 1901); **22**: *Recurvoides* sp.; **23**, **24**: *Thalmannammina subturbinata* (Grzybowski, 1898); **25**: *Trochamminoides proteus* (Karrer, 1866); **26**: *Trochamminoides variolarius* (Grzybowski, 1898); All from sample PEG 36, length of scale bars 0.1 mm.

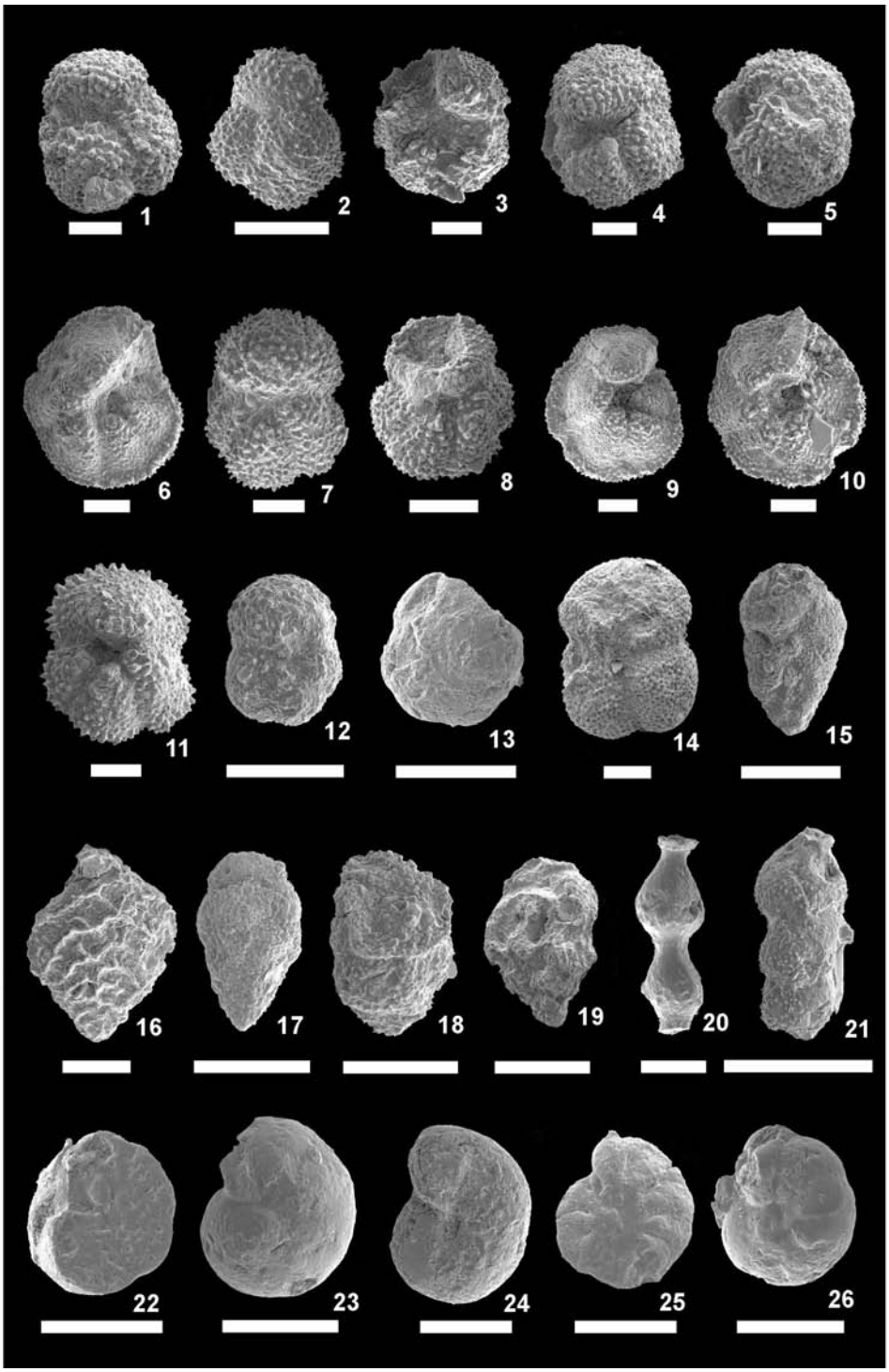

Figure A3.20 ▲
Planktic and calcareous benthic foraminifera
1: *Acarinina coalingensis* (Cushman & Hanna, 1927); **2**: *Acarinina* cf. *esnaensis* (LeRoy, 1953); **3**: *Acarinina nitida* (Martin, 1943); **4**: *Acarinina soldadoensis* (Brönnimann, 1952); **5**: *Acarinina subsphaerica* (Subbotina, 1947); **6**: *Morozovella acuta* (Toulmin, 1941); **7**: *Morozovella aequa* (Cushman & Renz, 1942); **8**: *Morozovella apanthesma* (Loeblich & Tappan, 1957); **9**: *Morozovella gracilis* (Bolli, 1957); **10**: *Morozovella occlusa* (Loeblich & Tappan, 1957); **11**: *Morozovella subbotinae* (Morozova, 1939); **12**: *Parasubbotina varianta* (Subbotina, 1953); **13**: *Planorotalites pseudoscitula* (Glaessner, 1937); **14**: *Subbotina triangularis* (White, 1928); **15**: *Chiloguembelina trinitatensis* (Cushman & Renz, 1942); **16**: *Aragonia velascoensis* (Cushman, 1925); **17**: *Bolivina midwayensis* Cushman, 1936; **18**: *Bulimina* sp. (?cf. *bradbury* Martin, 1943); **19**: *Bulimina* cf. *trinitatensis* Cushman & Jarvis, 1928; **20**: *Stilostomella gracillima* (Cushman, 1933); **21**: *Stilostomella subspinosa* (Cushman, 1943); **22**, **23**: *Cibicidoides tuxpamensis* (Cole, 1928); **24**: *Gavelinella danica* (Brotzen, 1940); **25**: *Gavelinella* cf. *micra* (Bermudez, 1949); **26**: *Hanzawaia cushmani* (Nuttall, 1930); All from sample PEG 05, except 16 (PEG 04), length of scale bars 0.1 mm.